Chemical Engineering Journal 166 (2011) 391–400

Contents lists available at ScienceDirect

Chemical Engineering Journal

journal homepage: www.elsevier.com/locate/cej

Fabrication and characterization of hierarchical ZSM-5 zeolites by using organosilanes as additives

Ya-Ping Guo*, Hai-Jin Wang, Ya-Jun Guo*, Li-Hua Guo, Lian-Feng Chu, Cui-Xiang Guo

Department of Chemistry, Shanghai Normal University, 100 Guilin Rd., Shanghai 200234, China

ARTICLE INFO

Article history:
Received 6 July 2010
Received in revised form
26 September 2010
Accepted 20 October 2010

Keywords:
ZSM-5 zeolites
Hierarchical structure
Mesopore
Nanocrystal
Organosilane

ABSTRACT

Two synthesis strategies were utilized to fabricate hierarchical ZSM-5 zeolites by using 3-aminopropyltrimethoxysilane (APTMS), N-[3-(trimethoxysilyl)propyl] ethylenediamine (TMPED) and (N,N-diethyl-3-aminopropyl)trimethoxysilane (DATMS) as additives. The first synthesis strategy comprises three steps: preparation of the zeolite precursors, anchoring of the organosilanes onto the zeolite precursors, and formation of the hierarchical ZSM-5 zeolites. The second synthesis strategy is similar to the above strategy, except that the organosilanes are directly added into the original reaction solution. The hierarchical ZSM-5 zeolites exhibit an ellipsoidal shape with a long-axis length of ~750 nm and short-axis length of ~550 nm, which include lots of nanocrystals with a size of ~25 nm. The aggregation of the nanocrystals leads to forming mesopores with a size of 2.8 nm and supermicropores with a size of 1.4 nm or 1.8 nm. However, the ZSM-5 zeolites prepared without using the organosilanes as additives exhibit an irregular shape with a broad particle size distribution. Benzene alkylation with ethene was carried out with ZSM-5 zeolites in a fixed bed reactor. The results show that the hierarchical ZSM-5 zeolites exhibit the higher C_2H_4 conversion and ethylbenzene selectivity than the conventional ZSM-5 zeolites.

1. Introduction

Ethylbenzene (EB) is an important intermediate in the production of polystyrene, and its worldwide capacity is about 23 million tonnes per year [1,2]. Benzene alkylation with pure ethene is a vital step in the synthesis of EB. Dalian Institute of Chemistry Physics in China has developed the synthetic technology of converting benzene with dilute ethene in FCC (fluid catalytic cracking) off-gas, without purification [1,3]. ZSM-5 zeolite catalyst exhibits the excellent catalytic performance in the production of EB. The great success of ZSM-5 catalysis may be attributed to the presence of well-defined microporous structure that is responsible for the molecular sieve and shape-selectivity [4–8]. However, the sole presence of micropores with aperture diameters below 1 nm, often imposes diffusion limitations that adversely affect catalytic activity, especially when the diffusion rates of reagents and reaction products are significantly slower than reaction rates [6,9].

In order to overcome the diffusion limitations, several strategies have been developed in recent years. The first strategy is to reduce the crystal size of zeolite catalysts [10–12]. The scaling down of zeolite crystals from the micrometer to the nanometer scale leads to decreasing diffusion path lengths and thus improving molecular diffusion [10]. However, this method is limited owing to the difficult separation of nanosized zeolite crystals from the reaction system. The second strategy is to introduce mesopores in the microporous materials through template methods or desilication processes [13–17]. Micropores in zeolites exhibit shape-selectivity for guest molecules, while mesopores act as channels for reactants to the active sites in micropores. Usually, carbon particles [18], carbon nanotubes [19], colloid-imprinted carbons [20], mesoporous carbons [21,22], amphiphilic organosilane surfactant [23], silylated polyethylenimine [24], CTAB [25], cationic polymers [13] have been used as mesopore-forming agents to fabricate mesoporous zeolites. In addition, desilication is an efficient method to create intracrystalline mesoporosity in MFI-type zeolites [26–28].

The third strategy is based on the aggregation of zeolite nanocrystals to form hierarchical ZSM-5 particles [9,29]. These materials possess the advantages of both nanocrystalline zeolites and mesoporous zeolites. On the one hand, owing to the presence of nanocrystals, the external surface areas are at least 3 times greater than those of conventional zeolite crystals [29]. On the other hand, the supermicropores or mesopores among the nanocrystals assist the mass transport of the reactants and products to and from the active sites [30]. Serrano et al. introduced a novel strategy to fabricate hierarchical ZSM-5 zeolites, which includes the following steps: precrystallization of the zeolite synthesis gel, functionalization of the zeolite seeds by organosilanes, crystallization of the functionalized seeds, and calcinations to remove the structure-directing and surface-silanizing agents [29,31,32]. Recently, we

* Corresponding authors. Tel.: +86 21 64321951; fax: +86 21 64321951.
E-mail addresses: ypguo@shnu.edu.cn (Y.-P. Guo), guoyajun2000@yahoo.com.cn (Y.-J. Guo).

1385-8947/$ – see front matter © 2010 Elsevier B.V. All rights reserved.
doi:10.1016/j.cej.2010.10.057

found that the hierarchical ZSM-5 zeolites could be fabricated by direct addition of the organosilanes into the original solution without the precrystallization step.

The main aim of this work, as compared with that by Serrono et al. [29,31,32], are as followed: (i) the present work reveals that the precrystallization step of the zeolite synthesis gel is not the precondition for the fabrication of the hierarchical ZSM-5 zeolite ellipsoids; (ii) the effects of the organosilanes on the formation of the ellipsoids has been discussed deeply; (iii) the catalytic activities of the hierarchical ZSM-5 zeolites during the alkylation of benzene with ethene have been investigated.

2. Experimental

2.1. Materials

Tetraethyl orthosilicate (TEOS) and aluminum isopropoxide (AIP) were purchased from Sinopharm Chemical Reagent Co., Ltd. Tetrapropylammonium hydroxide (TPAOH) was purchased from Shanghai Nuotai Chem Co., Ltd. N-[3-(Trimethoxysilyl)propyl] ethylenediamine (TMPED) was purchased from Shanghai Jingchun Reagent Co., Ltd. 3-Aminopropyltrimethoxysilane (APTMS) and (N,N-diethyl-3-aminopropyl)trimethoxysilane (DATMS) were purchased from Zhangjiagang Guotai-Huarong New Chemical Materials Co., Ltd. The structure formulas of APTMS, TMPED and DATMS are shown in Fig. 1.

2.2. Preparation of ZSM-5 zeolites

ZSM-5 zeolite samples were prepared according to the literature procedure [29]. TEOS, AIP, TPAOH and distilled water were used as original reagents to prepare a precursor solution of ZSM-5 zeolites with the following molar composition: 1 Al_2O_3:60 SiO_2:11.5 TPAOH:1500 H_2O. The solution was precrystallized under reflux with stirring at 90 °C for 20 h. Then, the zeolite precursors were functionalized by reaction with APTMS, TMPED, and DATMS (5 mol% in regards to the silica content in the gel) at 90 °C for 6 h, respectively. Finally, the resulting solution was subjected to crystallization in a teflon-lined stainless-steel autoclave at 170 °C for 5 days. The precipitations were separated by centrifugation, washed with distilled water, dried at 110 °C, and calcined at 550 °C for 4 h. The obtained samples by using APTMS, TMPED and DATMS as additives were denoted as ZSM-5A, ZSM-5T and ZSM-5D, respectively.

The second synthesis route to fabricate hierarchical ZSM-5 zeolites was similar to the above route. The only difference was that APTMS, TMPED or DATMS were added directly into the precursor solution, and then were stirred under reflux at 90 °C for 26 h. The other synthesis procedures including crystallization of the zeolite precursors and calcinations of products were not changed. The products by using APTMS, TMPED and DATMS as additives were denoted as ZSM-5AP, ZSM-5TP and ZSM-5DP, respectively. In addition, a reference ZSM-5 zeolite was synthesized under the same conditions but without the addition of the organosilanes. The sample was denoted as ZSM-5N.

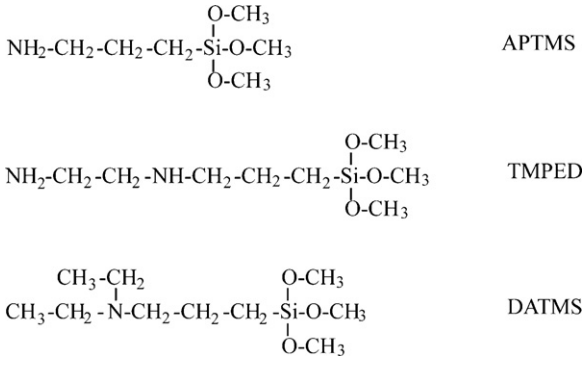

Fig. 1. The structure formulas of organosilanes including APTMS, TMPED and DATMS.

2.3. Characterization

The morphologies of samples were investigated by scanning electron microscopy (SEM, JSM-6380LV) and transmission electron microscopy (TEM, JEOL2100) with electron diffraction (ED). The crystalline phases of samples were examined with X-ray powder diffraction (XRD, D/max-III C) using CuKα radiation. The relative crystallinity of samples was calculated by using MDI JADE 5.0 software. The crystallinity of samples was evaluated according to the formula: crystallinity = $(X/Y) \times 100\%$, where X is the net area of diffracted peaks, and Y is the net area of diffracted peaks + background area [33]. Fourier transform infrared spectra (FTIR, Nicolet 5DX) were collected at room temperature by using the KBr pellet technique working in the range of wavenumbers 4000–400 cm^{-1} at a resolution of 2 cm^{-1} (number of scans ~60). N_2 adsorption–desorption isotherms were measured with an automatic surface area and porosity analyzer (AUTOSORB-1-C, Quantachrome) at 77 K. The pore volume and pore-size distributions were derived from the adsorption branches of the isotherms using nonlocal density functional theory (NLDFT).

2.4. Catalytic performance of ZSM-5 zeolites

The ZSM-5A, ZSM-5T, ZSM-5D and ZSM-5N used pseudoboehmite as the binder in a weight ratio of 70:30 (zeolite/pseudoboehmite), and formed into catalyst extrudates. Benzene alkylation with ethene was carried out with 3.0 g catalyst (containing zeolite and pseudoboehmite) in the fixed bed reactor. After flushing with N_2 with a flow rate of 300 ml/min, the reactants comprising benzene and ethene with a molar ratio of 5:1 were introduced into the reactor at a weight space velocity of 0.5 h^{-1} under a pressure of 1.0 MPa. After reaction for 2 h at 350 °C, the products were analysed by gas chromatography with FFAP capillary column and FID.

3. Results and discussion

3.1. Structure of hierarchical ZSM-5 zeolites

Fig. 2 shows the XRD patterns of the ZSM-5 zeolites prepared by hydrothermal method with or without organosilanes as organic additives. They all exhibit the characteristic diffraction peaks occurred at 2θ of 7.92°, 8.80°, 14.78°, 23.18°, 23.90°, 24.40°, which are exclusively indexed to the structure of MFI topology (JCPDS no. 42-0024). The broadening of the diffraction lines indicates the presence of nanometer-sized crystals. These samples exhibit good crystallinity, which is identified quantitatively by using MDI JADE 5.0 software, as shown in Table 1. It is noted that the crystallinities of zeolites are related to the organosilanes, and the order is as follows: ZSM-5A > ZSM-5T > ZSM-5N > ZSM-5D.

The zeolite framework vibrations and silanol groups were characterized by FTIR spectra, as shown in Fig. 3. The absorption bands at 1230 cm^{-1} (external asymmetric stretch), ~1100 cm^{-1} (internal asymmetric stretch), 798 cm^{-1} (external symmetric stretch) and 459 cm^{-1} (T-O bend) are corresponding to siliceous materials [9]. The ZSM-5 zeolites display the characteristic bands at 3682 cm^{-1} due to isolated silanol groups and at 3474 cm^{-1} due to framework Al–OH (Brønsted acid sites). The characteristic band of the double five rings of the MFI-type zeolites is located at 549 cm^{-1} [9], which

Table 1
Crystallinity, textural properties of the ZSM-5 zeolites.

Samples	Size of nanoparticle[a] (nm)	Size of agglomerate (nm)	Crystallinity (%)	Pore size[b] (nm)	S_{BET}[c] (m^2/g)	S_{MIC}[d] (m^2/g)	V_{MIC}[d] (cm^3/g)
ZSM-5N	42 ± 14	/[e]	80.07	1.4/1.8/2.8	379	229	0.101
ZSM-5A	26 ± 6	726 ± 104/552 ± 68[f]	87.73	1.4/1.8/2.8	606	269	0.084
ZSM-5T	28 ± 6	728 ± 94/558 ± 58[f]	80.34	1.4/1.8/2.8	434	233	0.108
ZSM-5D	22 ± 5	722 ± 105/550 ± 74[f]	73.26	1.4/1.8/2.8	456	213	0.090

[a] Data are represented as mean ± standard deviation; $n = 30$.
[b] Data are determined by applying the NLDFT method.
[c] Data are determined by applying the multi-point BET.
[d] Data are determined by applying the *t*-plot method.
[e] Data are determined difficultly due to the irregular morphology of ZSM-5N agglomerates.
[f] Length data for long axis (left) and short axis (right) of ellipoids are represent as mean ± standard deviation; $n = 20$.

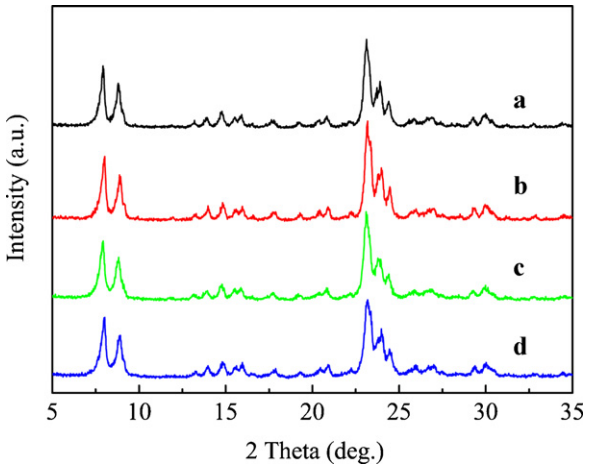

Fig. 2. XRD patterns of the different ZSM-5 zeolites: (a) ZSM-5N, (b) ZSM-5A, (c) ZSM-5T, and (d) ZSM-5D.

can be used to determine the crystalline degree of the samples [21]. The high intensity of the 549 cm^{-1} band suggests that the ZSM-5A, ZSM-5T, ZSM-5N and ZSM-5D have great crystalline degree, as confirmed by the XRD patterns (Fig. 2 and Table 1). The characteristic band of silanol groups is observed at 972 cm^{-1} [10]. It is noted that the intensity of silanol groups in the ZSM-5A, ZSM-5T and ZSM-5D is greater than that in the ZSM-5N (Fig. 3), which may be related to the surface areas of zeolites (Table 1).

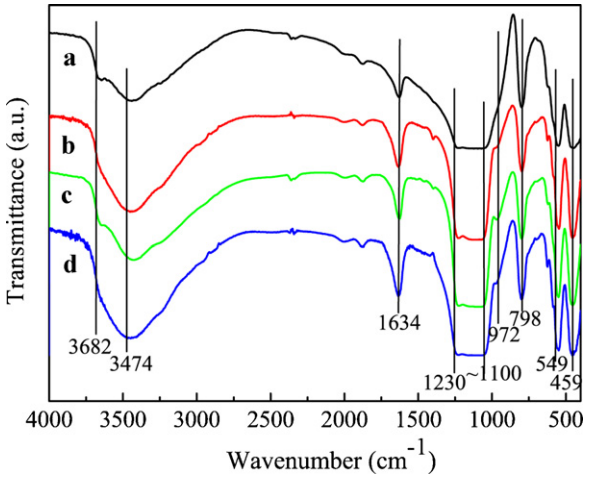

Fig. 3. FTIR spectra of the different ZSM-5 zeolites: (a) ZSM-5N, (b) ZSM-5A, (c) ZSM-5T, and (d) ZSM-5D.

3.2. Morphology and porous structure of hierarchical ZSM-5 zeolites

Fig. 4 shows the SEM images of the different ZSM-5 zeolites. The shape of the ZSM-5N is not very regular, which consists of large particles and lots of small particles. The particle size of the small particles is 42 ± 14 nm (Fig. 5a and Table 1), while that of the large particles is 400 ± 200 nm (Figs. 4a and 5b). The ED pattern in Fig. 5b indicates that the ZSM-5N large particle is single crystal with the [0 1 0] zone axis. Interestingly, the organosilanes have great effects on the morphologies of the ZSM-5 zeolites (Fig. 4). The ZSM-5 zeolites prepared by using the organosilanes as additives exhibit ellipsoidal shape with a long-axis length of ~750 nm and short-axis length of ~550 nm (Fig. 4 and Table 1), which are formed by the aggregation of lots of nanocrystals with a particle size of ~25 nm (Fig. 6 and Table 1). To some extent, these adjacent nanocrystals exhibit the same crystalline orientations, which may be attributed to some kind of oriented organosilane absorption due to the MFI-type anisotropy (Fig. 6b, d and f). However, if no organosilanes are added into the reaction system, the as-obtained ZSM-5N nanocrystals do not exhibit the same crystalline orientations.

Fig. 7 shows the nitrogen adsorption–desorption isotherm and the corresponding pore size distributions of ZSM-5 zeolites. The curves in Fig. 7a, c, e and g are identified as Type IV isotherms with Type H3 hysteresis loops [32]. The Type H3 loop, which does not exhibit any limiting adsorption at high P/P_o, is attributed to the aggregates of the ZSM-5 nanocrystals giving rise to slit-shaped pores in random arrangement without precise orientation ordering (Fig. 6) [34]. The supermicropores and mesopores exist in the intercrystalline void, and cannot be observed in the individual crystals (Figs. 5 and 6). This result can be confirmed by the low-angle XRD patterns. No characteristic diffraction peaks corresponding to ordered mesopores are observed in the low-angle XRD patterns (Fig. S1). Fig. 7 shows that the adsorbed amount of N_2 at both low and intermediate relative pressures for the ZSM-5A, ZSM-5T and ZSM-5D is greater than that for the ZSM-5N, which suggests that the ZSM-5 zeolites prepared by using the organosilanes as additives possess higher porosities and surface areas than the ZSM-5N. For the ZSM-5A, ZSM-5T and ZSM-5D, the mesopores with a pore size of 2.8 nm and the supermicropores with a pore size of 1.4 nm or 1.8 nm are observed in the DFT pore size distributions, while the intensity of the mesopores and supermicropores is low for the ZSM-5N (Fig. 7). The supermicropores and mesopores exist among the nanocrystals, which are confirmed by TEM images (Fig. 6). Table 1 shows that the ZSM-5A, ZSM-5T and ZSM-5D zeolites possess the greater BET areas than the ZSM-5N zeolites. The reasons are attributed to the following two reasons. Firstly, the presence of nanocrystals in the hierarchical ZSM-5 zeolites increases the external surface areas, which are at least 3 times greater than those of conventional zeolite crystals [29]. Secondly, besides the micropores, the mesopores and supermicropores among the nanocrystals contribute the great BET areas for the hierarchical ZSM-5 zeolites in

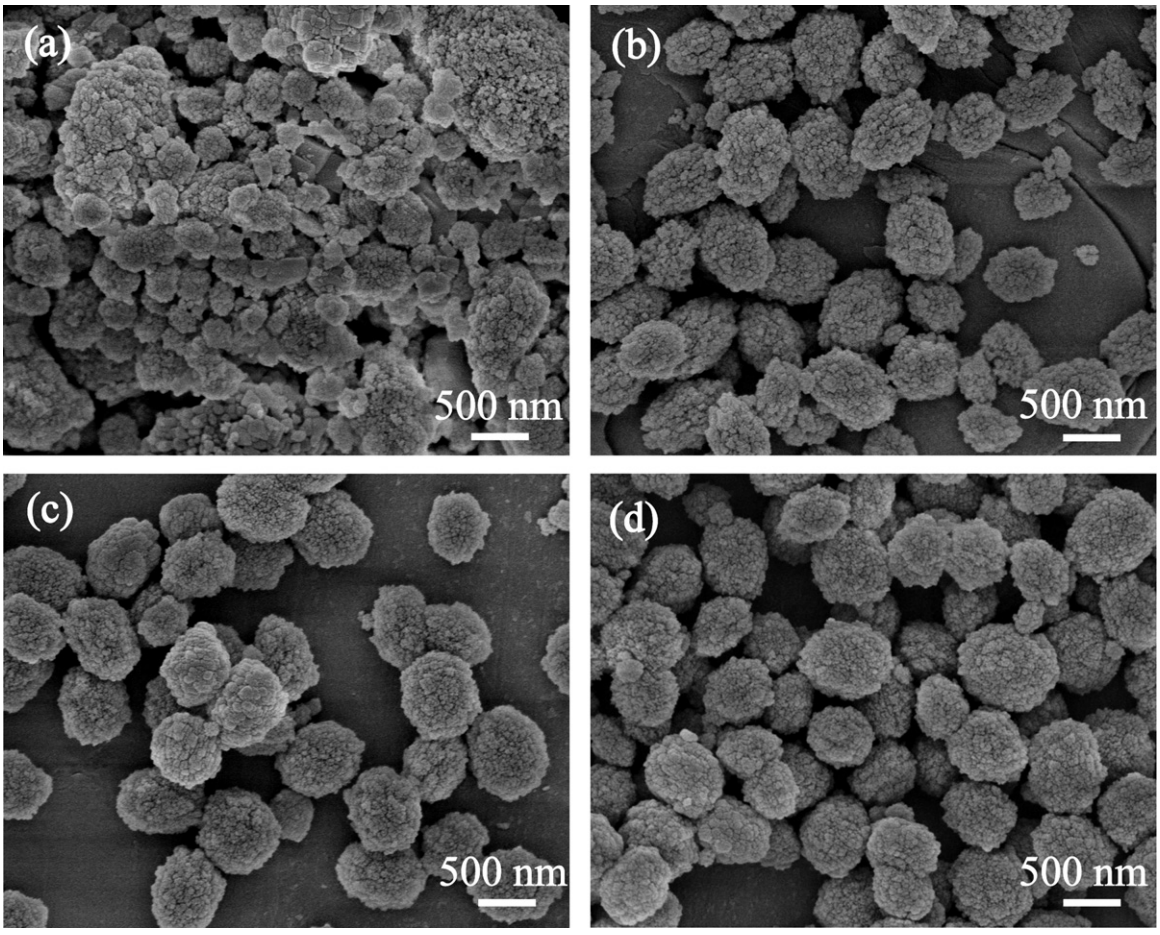

Fig. 4. SEM images of the different ZSM-5 zeolites: (a) ZSM-5N, (b) ZSM-5A, (c) ZSM-5T, and (d) ZSM-5D.

comparison with the purely microporous counterparts. The large surface areas of the ZSM-5A, ZSM-5T and ZSM-5D provide more silanol sites that are available for chemical functionalization than the ZSM-5N, as shown in Fig. 3.

3.3. Formation mechanism of hierarchical ZSM-5 zeolites

The organosilanes such as TMPED, APTMS and DATMS have great effects on the ZSM-5 zeolites (Fig. 4). Serrano et al. have proposed that the hierarchical ZSM-5 zeolites are originated from silanized protozeolitic nanounits, which includes the following three stages: (i) a precursor gel containing protozeolitic MFI nanounits is formed from clear solution (precrystallization step); (ii) the silanization agents are anchored onto the zeolite seeds (silanization step); and (iii) the samples are crystallized under hydrothermal conditions (crystallization step) [32]. According to the above formation mechanism, the formation of protozeolitic MFI nanounits in the precrystallization step is precondition.

Is the precrystallization step precondition for the fabrication of the hierarchical ZSM-5 zeolites? The TEM images of the precur-

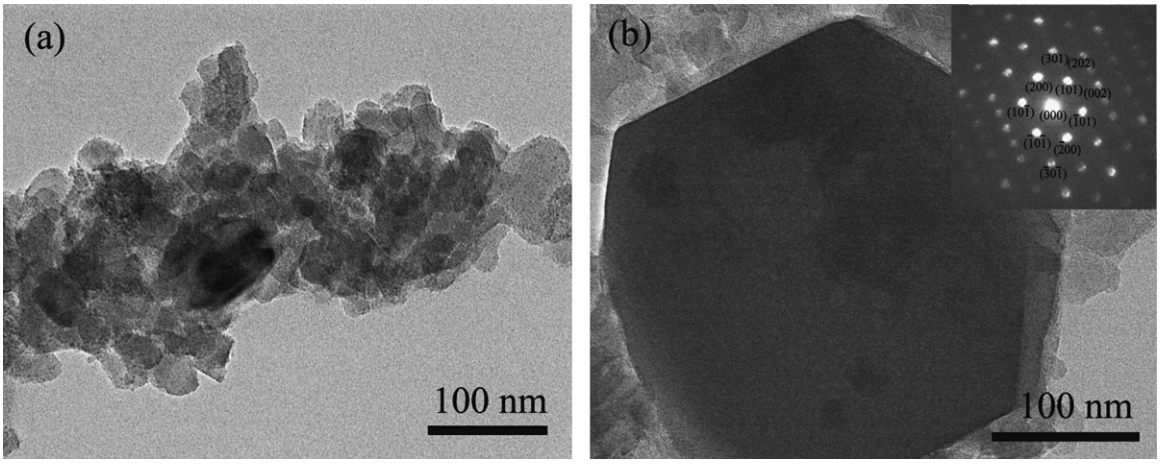

Fig. 5. TEM images of ZSM-5N. The inset shows the corresponding ED pattern.

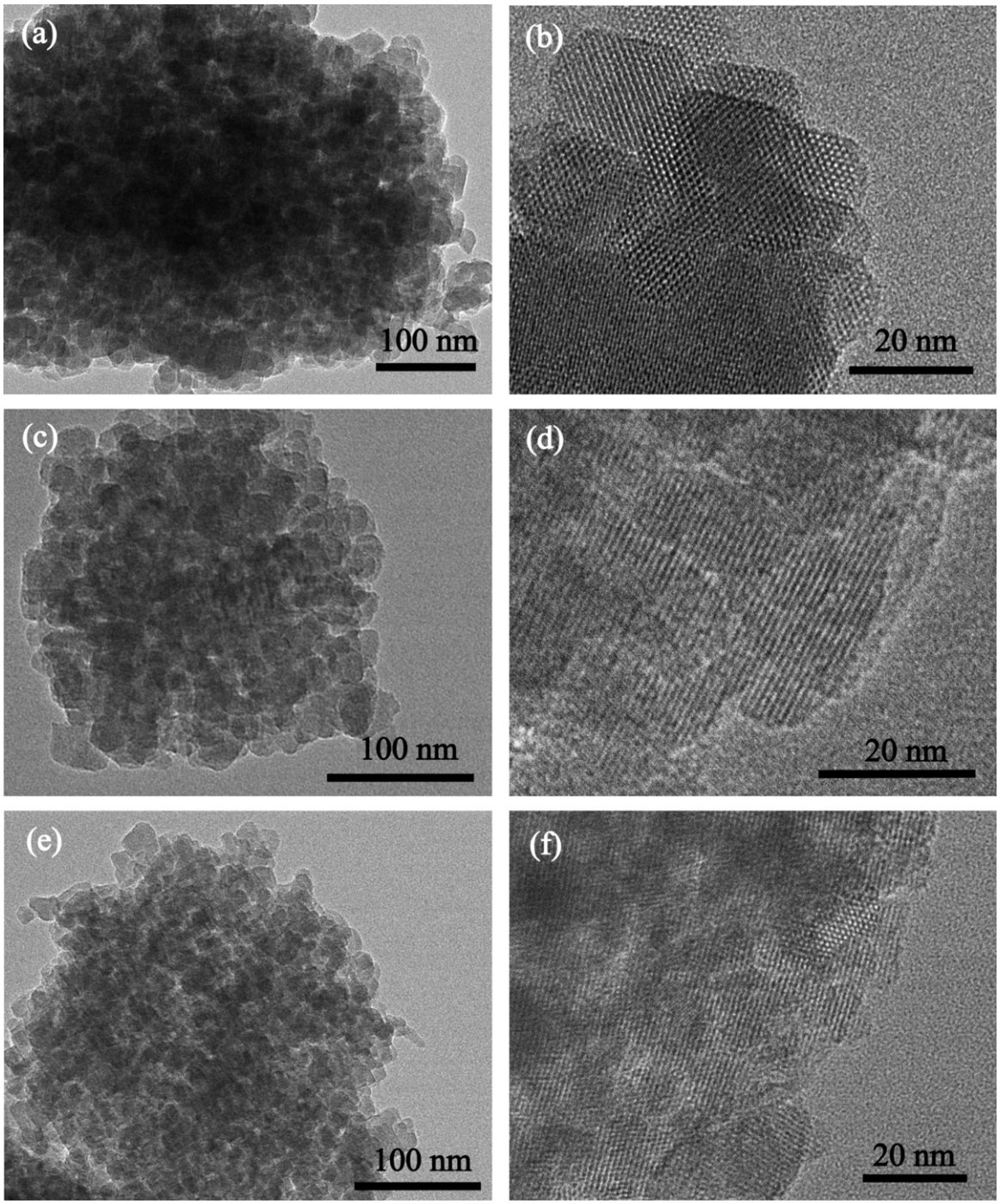

Fig. 6. TEM images of the different ZSM-5 zeolites: (a and b) ZSM-5A, (c and d) ZSM-5T, and (e and f) ZSM-5D.

sor sol–gel mixture are performed, as shown in Fig. 8. The sol–gel mixture is prepared from the mixing solution of the TEOS, AIP, TPAOH and distilled water after precrystallization under reflux at 90 °C for 20 h, as described in Section 2. Fig. 8a shows that the samples exhibit gelatinous properties. At the same time, some hollow microspheres with the particle size of 1–3 μm are obtained (Fig. 8b), which may be formed by using air bubbles as templates during the precrystallization step. The corresponding ED pattern confirms further that the samples are amorphous and no characteristic diffraction rings (or diffraction spots) of ZSM-5 zeolites are obtained (inset, Fig. 8b). Based on the results of the TEM images and ED pattern, it can be concluded that the precursor sol is mainly the congeries of TEOS, AIP, TPAOH and distilled water.

In order to confirm further the importance of the precystallization step, the organosilanes are directly added into the precursor solution without the precrystallization step. Interestingly, the ZSM-5AP, ZSM-5TP and ZSM-5DP exhibit the hierarchical structure (Figs. 9 and 10), which are similar to the ZSM-5A, ZSM-5T and ZSM-5D (Figs. 4 and 6). The ZSM-5 particles with a long-axis length of ~750 nm and short-axis length of ~550 nm are also composed of many nanoparticles with a size of ~25 nm (Figs. 9 and 10). The ED pattern demonstrates that the ultrasmall primary units are single crystals (Fig. 10b). The phases of the samples are characterized by using the XRD patterns, as shown in Fig. 11. The ZSM-5AP, ZSM-5TP and ZSM-5DP all exhibit the characteristic diffraction peaks of ZSM-5 crystalline occurred at 2θ of 7.92°, 8.80°, 14.78°, 23.18°, 23.90°,

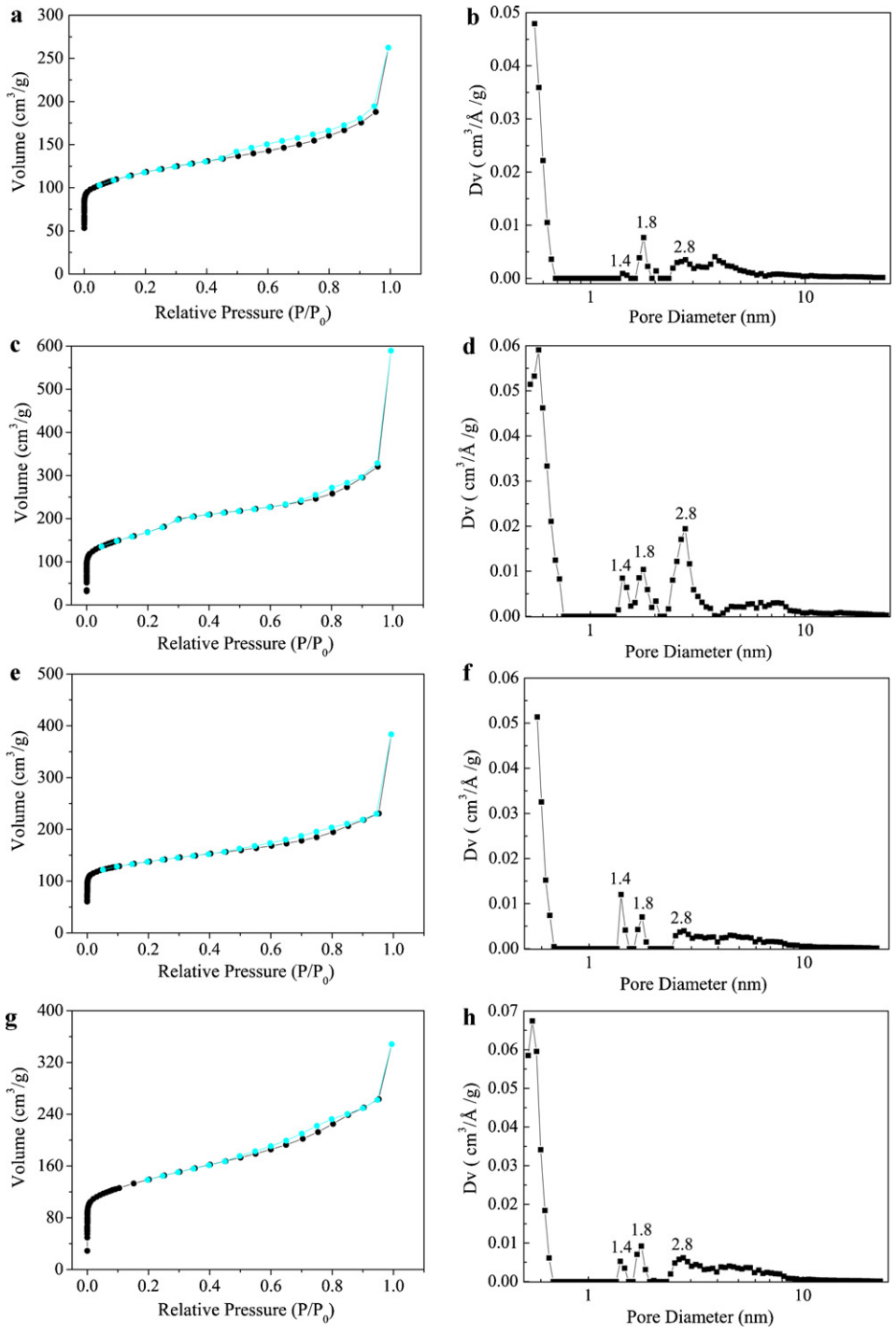

Fig. 7. Nitrogen adsorption–desorption isotherms and DFT pore size distribution of the different ZSM-5 zeolites: (a and b) ZSM-5N, (c and d) ZSM-5A, (e and f) ZSM-5T, and (g and h) ZSM-5D.

24.40°. The crystallinities of the ZSM-5AP, ZSM-5TP and ZSM-5DP are 82.7%, 79.3% and 76.4%, respectively, which are similar to those of the ZSM-5A, ZSM-5T and ZSM-5D (Table 1). These results indicate that the addition sequence of the organosilanes into the precursor solution does not change the hierarchical structure and crystallinity of the zeolites. The precrystallization step is not precondition for the fabrication of the hierarchical ZSM-5 zeolites.

Based on the above results, the formation mechanism of hierarchical ZSM-5 zeolites can be proposed, as shown in Fig. 12. The first synthetic pathway comprises three steps. Firstly, after reflux at 90 °C for 20 h, the clear solution including TPAOH, TEOS, AIP and H_2O is converted to a sol–gel reaction mixture, which can be used as a zeolite precursor (Fig. 12a and b). The TEM images indicate that the zeolite precursor exhibits gelatinous properties (Fig. 8), suggesting that the zeolite precursor may be congeries of TEOS, AIP, TPAOH and water. Secondly, the organosilanes such as TMPED, APTMS and DATMS are added into the sol–gel reaction mixture, and are stirred under reflux at 90 °C for 6 h. The $-SiO_3$ groups in the organosilanes allow them to be integrated into the surfaces of zeolite precursors through covalent Si–O–Si linkages (Fig. 12d and f) [24]. In addition, the hydrogen bonding interactions cannot be ignored between $-NH_2$ groups in the organosilanes and silanol

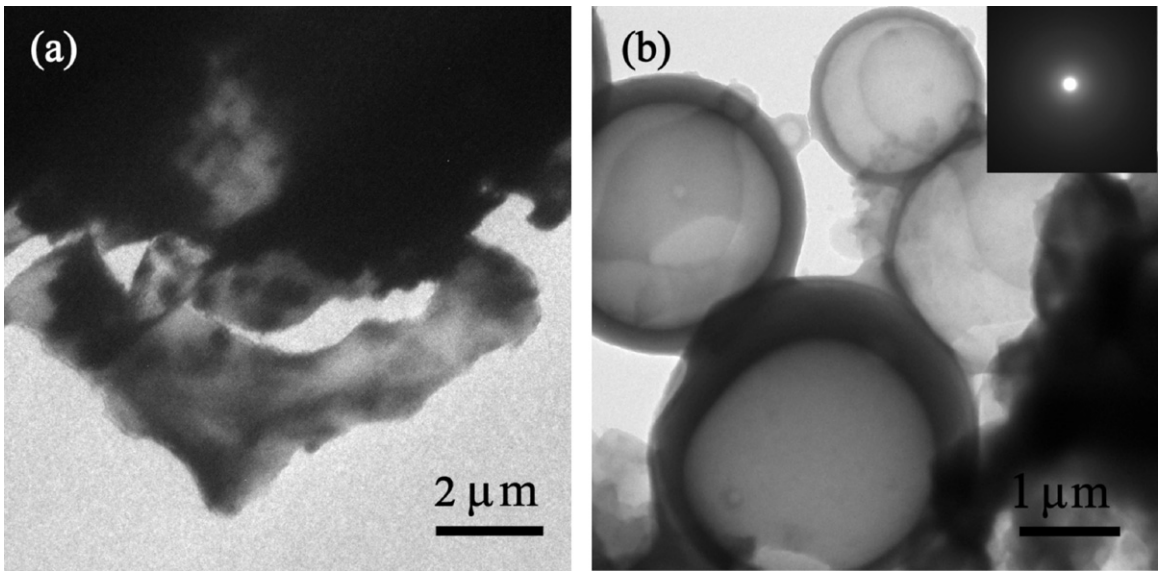

Fig. 8. (a and b) TEM images of the samples obtained from the mixed solution of TEOS, AlP, TPAOH and distilled water after precrystallization under reflux with stirring at 90 °C for 20 h. The inset shows the corresponding ED pattern.

groups in the zeolite precursors. The silanol groups are remained even after calcinations at 550 °C for 4 h (Fig. 3). Thirdly, as the zeolite precursors are crystallized in the teflon-lined stainless-steel autoclave at 170 °C, the organosilanes become nanocrystal-segregated. Calcination of the samples removes the organosilanes and TPAOH, resulting in the formation of the hierarchical ZSM-5 zeolites with uniform intercrystal supermicropores or mesopores.

The second synthetic pathway of the hierarchical ZSM-5 zeolites comprises two steps, as shown in Fig. 12. The only difference as compared with the first synthetic pathway is that the organosi-

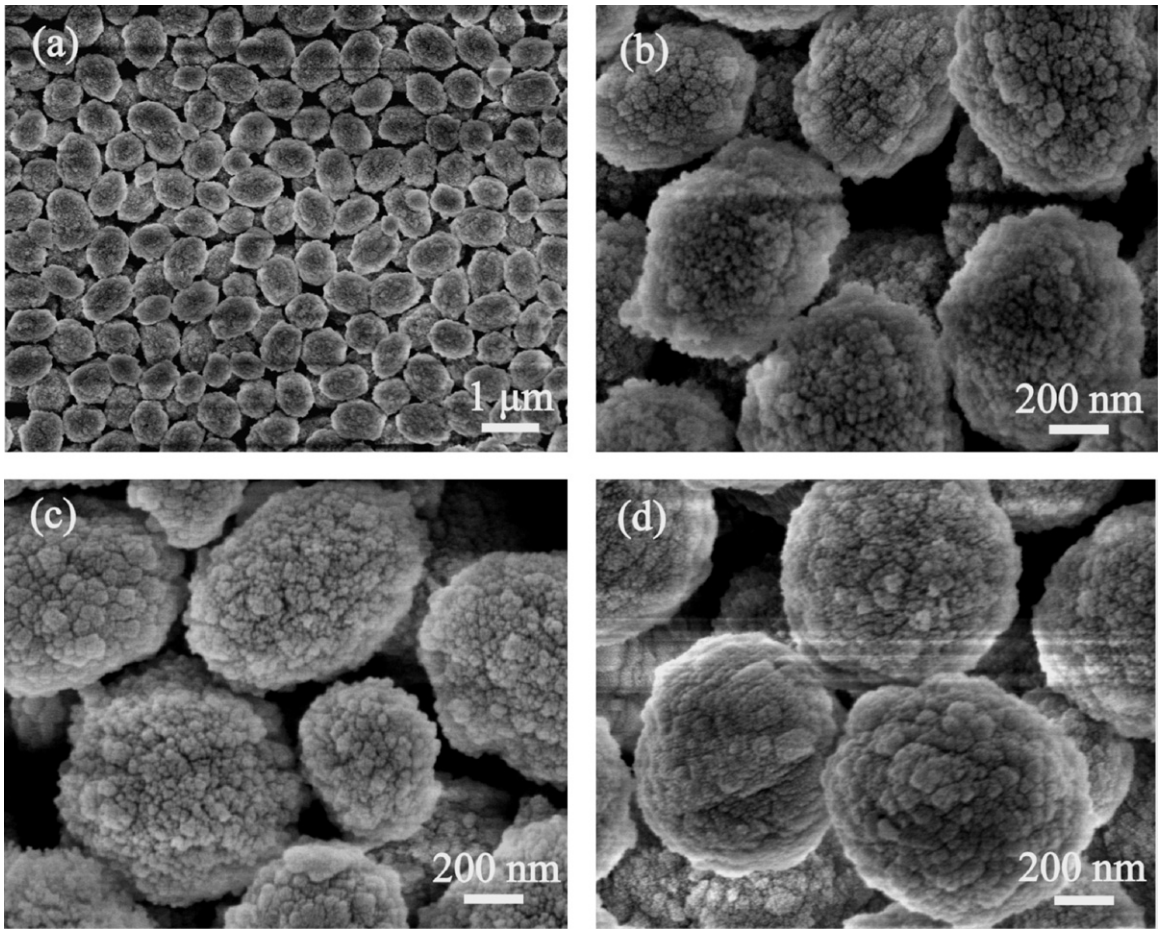

Fig. 9. SEM images of the different ZSM-5 zeolites: (a and b) ZSM-5AP, (c) ZSM-5TP, and (d) ZSM-5DP.

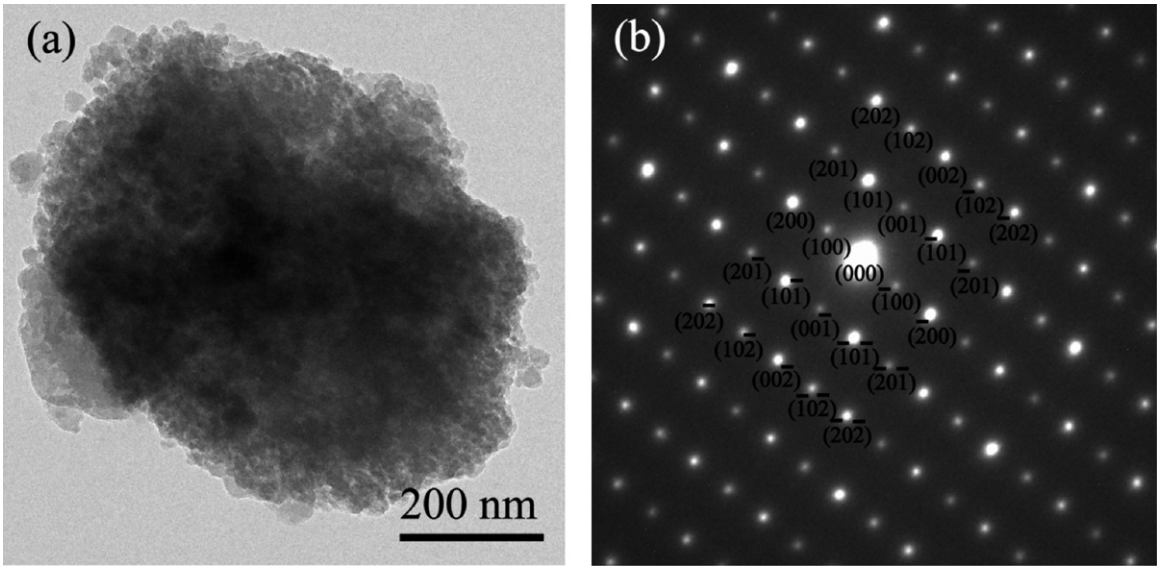

Fig. 10. (a) TEM images and (b) ED pattern of ZSM-5AP.

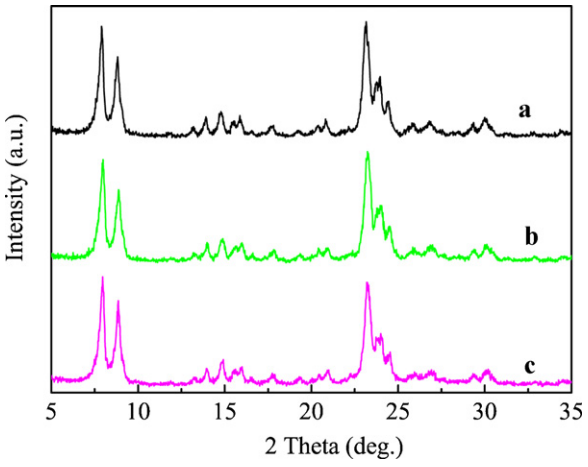

Fig. 11. XRD patterns of the different ZSM-5 zeolites: (a) ZSM-5AP, (b) ZSM-5TP, and (c) ZSM-5DP.

lanes are directly added into the original solution with TPAOH, TEOS, AIP and water. The mixture solution is stirred under reflux at 90 °C for 26 h. As the sol–gel reaction mixture forms, the organosilanes are anchored onto the surfaces of zeolite precursors through the covalent Si–O–Si linkages and hydrogen bonding interactions (Fig. 12c and d). The XRD patterns (Figs. 2 and 11) and SEM images (Figs. 4 and 9) indicate that the phase structure and morphology of the ZSM-5 zeolites prepared by the second pathway are similar to those by the first pathway.

3.4. Effect of organosilanes on hierarchical ZSM-5 zeolites

The organosilanes have great effects on the morphologies of the ZSM-5 zeolites. The hierarchical ZSM-5 zeolites are obtained if the organosilanes are added into the reaction system by the above two different pathways (Figs. 4 and 9). However, the shapes of the ZSM-5N prepared without the organosilanes as additives are irregular (Figs. 4a and 5). How do the organosilanes affect the hierarchical structure of ZSM-5 zeolites? The reasons may be attributed to the following two possibilities: (i) the organosilanes which are anchored on the surfaces of zeolite precursors through the covalent

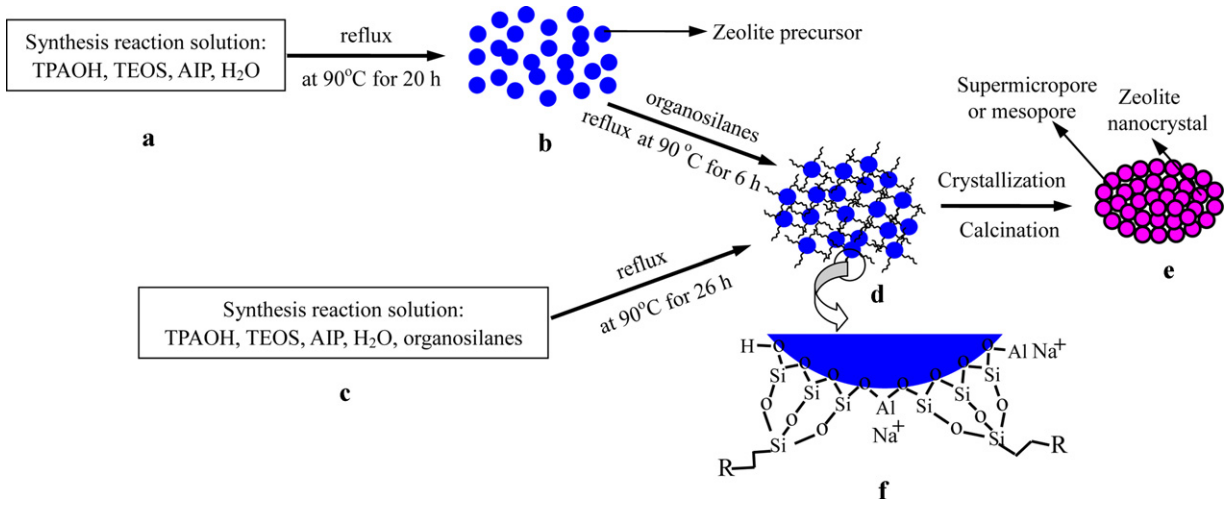

Fig. 12. Schematic representation of the formation process of hierarchical ZSM-5 zeolites.

Table 2
Catalytic activity of the ZSM-5 zeolites.

Samples	C_2H_4 conversion (%)[a]	EB selectivity (%)[a]
ZSM-5N	54.4 ± 0.2	88.7 ± 0.2
ZSM-5A	56.4 ± 0.1	91.1 ± 0.2
ZSM-5T	55.4 ± 0.2	91.6 ± 0.2
ZSM-5D	55.5 ± 0.1	91.8 ± 0.2

[a] Data are represented as mean ± standard deviation; $n = 3$.

Si–O–Si linkages and hydrogen bonding interactions can hinder the growth of ZSM-5 crystals during crystallization step, so the size of the nanocrystals is only ~25 nm; (ii) since every organosilane molecular has three –$SiOCH_3$ groups, adjacent zeolite precursors can be connected by the Si–O–Si linkages. After crystallization and calcination, the hierarchical ZSM-5 particles including lots of nanocrystals are formed. In addition, the organosilanes as silica original may take part in the reaction, so the adjacent nanocrystals exhibit the same crystalline orientations to some extent.

Table 1 shows that different organosilanes have different effects on the crystallinity and textural properties of the ZSM-5 zeolites, which may be attributed to different molecular structure of the organosilanes. The molecular dimension of APTMS is smaller than that of TMPED and DATMS, although they have the same functional groups. The zeolite precursors can be covered with more APTMS due to the less steric hindrance than TMPED and DATMS, so the crystallization process cannot be affected by the adjacent zeolite precursors during the crystallization stage. Therefore, the obtained nanocrystals in the ZSM-5A particles are more dispersed (Fig. 6), and have greater external surface areas and crystallinity than the ZSM-5T and ZSM-5D (Table 1).

3.5. Catalytic performance of hierarchical ZSM-5 zeolites

Table 2 shows the catalytic performance of the ZSM-5 zeolites. From the catalytic performance over the ZSM-5N, a C_2H_4 conversion of 54.38% and EB selectivity of 88.75% are achieved. It is noted that the hierarchical ZSM-5 zeolites fabricated by using the organosilanes as additives, exhibit higher C_2H_4 conversion and EB selectivity than ZSM-5N (Table 2). The excellent catalytic activity of the ZSM-5A, ZSM-5T and ZSM-5D may be attributed to the hierarchical structure. The ZSM-5A, ZSM-5T and ZSM-5D exhibit the ellipsoidal shape with a long-axis length of ~750 nm and short-axis length of ~550 nm, which comprised lots of nanocrystals with a particle size of ~25 nm (Figs. 4 and 6). The aggregation of the nanocrystals induces the formation of the mesopores and supermicropores, and thus improves obviously the surface areas and active sites. However, the morphology of the ZSM-5N is irregular. The intensities of the supermicropores (and mesopores) and the surface areas of ZSM-5N are lower than those of the hierarchical ZSM-5 zeolites (Fig. 7 and Table 1).

The C_2H_4 conversion of the hierarchical ZSM-5 zeolites is greater than that of the ZSM-5N, which may be attributed to the following reasons. Firstly, the hierarchical ZSM-5 zeolites with the hybrid micro-/mesoporous structures possess the greater BET areas than ZSM-5N, which provide more active sites for the benzene alkylation with ethene. Secondly, it is well known that zeolitic catalysts suffer from intracrystalline diffusion limitations because of the molecular dimensions of the micropores [35]. The supermicropores and mesopores of the hierarchical ZSM-5 zeolites improve the diffusion rates of reagents and reaction products, and thus increase the catalytic activities. At the same time, the EB selectivity of the ZSM-5 zeolites may be associated with the supermicropores and mesopores [35]. The benzene alkylation reaction with ethene occurs not only within the micropores of zeolites but also on the surfaces. The EB selectivity is mainly attributed to the well-defined micropores that are responsible for the molecular sieve and shape-selectivity. The presence of the supermicropores and mesopores shorten the diffusion path length of reactants, so more benzene alkylation reactions occur within the micropores of zeolites rather than on the surfaces. Hence, the hierarchical ZSM-5 zeolites exhibit the higher EB selectivity than the ZSM-5N.

4. Conclusions

APTMS, TMPED and DATMS have been used as additives to fabricate the hierarchical ZSM-5 zeolites according to the following two synthesis strategies. The first synthetic pathway comprises three steps: preparation of the sol–gel reaction mixture as a zeolite precursor from the clear solution including TPAOH, TEOS, AIP and H_2O after reflux at 90 °C for 20 h, anchoring of the organosilanes onto the surfaces of zeolite precursors, and formation of the hierarchical ZSM-5 zeolites after crystallization and calcination. The second synthesis strategy is similar to the first synthesis strategy. The only difference is that the organosilanes are directly added into the original solution with TPAOH, TEOS, AIP and water. The XRD patterns, FTIR spectra and SEM images indicate that the addition sequence of the organosilanes into the reaction system does not change the hierarchical structure and crystallinity of the zeolites.

The organosilanes have great effects on the morphologies and porous structures of ZSM-5 zeolites. The ZSM-5 zeolites prepared by using organosilanes as additives present dispersed the ellipsoidal shape with a long-axis length of ~750 nm and short-axis length of ~550 nm, which include lots of nanocrystals with a size of ~25 nm. Moreover, these samples have hierarchical porous structures. Besides the micropores generated by the MFI channels, the mesopores with a pore size of 2.8 nm and supermicropores with a pore size of 1.4 nm or 1.8 nm are produced due to the aggregation of the zeolite nanocrystals. However, the ZSM-5 zeolites prepared without using organosilanes as additives exhibit irregular shape with a broad particle size distribution.

The catalytic performance of the ZSM-5 zeolites during the alkylation of benzene with ethene has been investigated in the fixed bed reactor at 350 °C. The results show that the hierarchical ZSM-5 zeolites exhibit higher C_2H_4 conversion and EB selectivity than the ZSM-5N.

Acknowledgements

This research was supported by Shanghai Science Committee (081658205).

Appendix A. Supplementary data

Supplementary data associated with this article can be found, in the online version, at doi:10.1016/j.cej.2010.10.057.

References

[1] Y. Song, S. Liu, Q. Wang, L. Xu, Y. Zhai, Coke burning behavior of a catalyst of ZSM-5/ZSM-11 co-crystallized zeolite in the alkylation of benzene with FCC off-gas to ethylbenzene, Fuel Process. Technol. 87 (2006) 297–302.
[2] L.M. Chua, T. Vazhnova, T.J. Mays, D.B. Lukyanov, S.P. Rigby, Deactivation of PtH-MFI bifunctional catalysts by coke formation during benzene alkylation with ethane, J. Catal. 271 (2010) 401–412.
[3] L. Xu, J. Liu, Q. Wang, S. Liu, W. Xin, Y. Xu, Coking kinetics on the catalyst during alkylation of fcc off-gas with benzene to ethylbenzene, Appl. Catal. A: Gen. 258 (2004) 47–53.
[4] M. Choi, K. Na, J. Kim, Y. Sakamoto, O. Terasaki, R. Ryoo, Stable single-unit-cell nanosheets of zeolite MFI as active and long-lived catalysts, Nature 461 (2009) 246–249.
[5] C.S. Cundy, P.A. Cox, The hydrothermal synthesis of zeolites: history and development from the earliest days to the present time, Chem. Rev. 103 (2003) 663–701.

[6] J. Pérez-Ramírez, C.H. Christensen, K. Egeblad, C.H. Christensen, J.C. Groen, Hierarchical zeolites: enhanced utilization of microporous crystals in catalysis by advances in materials design, Chem. Soc. Rev. 37 (2008) 2530–2542.
[7] K. Egeblad, C.H. Christensen, M. Kustova, C.H. Christensen, Templating mesoporous zeolites, Chem. Mater. 20 (2008) 946–960.
[8] C.H. Christensen, K. Johannsen, I. Schmidt, C.H. Christensen, Catalytic benzene alkylation over mesoporous zeolite single crystals: improving activity and selectivity with a new family of porous materials, J. Am. Chem. Soc. 125 (2003) 13370–13371.
[9] N. Chu, J. Yang, C. Li, J. Cui, Q. Zhao, X. Yin, J. Lu, J. Wang, An unusual hierarchical ZSM-5 microsphere with good catalytic performance in methane dehydroaromatization, Micropor. Mesopor. Mater. 118 (2009) 169–175.
[10] S.C. Larsen, Nanocrystalline zeolites and zeolite structures: synthesis, characterization, and applications, J. Phys. Chem. C 111 (2007) 18464–18474.
[11] A. Jawor, B.H. Jeong, E.M.V. Hoek, Synthesis, characterization, and ion-exchange properties of colloidal zeolite nanocrystals, J. Nanopart. Res. 11 (2009) 1795–1803.
[12] S. Ivanova, B. Louis, M.J. Ledoux, C. Pham-Huu, Autoassembly of nanofibrous zeolite crystals via silicon carbide substrate self-transformation, J. Am. Chem. Soc. 129 (2007) 3383–3391.
[13] F.S. Xiao, L.F. Wang, C.Y. Yin, K.F. Lin, Y. Di, J.X. Li, R.R. Xu, D.S. Su, R. Schlögl, T. Yokoi, T. Tatsumi, Catalytic properties of hierarchical mesoporous zeolites templated with a mixture of small organic ammonium salts and mesoscale cationic polymers, Angew. Chem. Int. Ed. 45 (2006) 3090–3093.
[14] H. Vinh-Thang, Q. Huang, A. Ungureanu, M. Eić, D. Trong-On, S. Kaliaguine, Structural and diffusion characterizations of steam-stable mesostructured zeolitic UL-ZSM-5 materials, Langmuir 22 (2006) 4777–4786.
[15] A. Malekian, H. Vinh-Thang, Q. Huang, M. Eić, S. Kaliaguine, Evaluation of the main diffusion path in novel micro-mesoporous zeolitic materials with the zero length column method, Ind. Eng. Chem. Res. 46 (2007) 5067–5073.
[16] J.C. Groen, T. Sano, J.A. Moulijn, J. Pérez-Ramírez, Alkaline-mediated mesoporous mordenite zeolites for acid-catalyzed conversions, J. Catal. 251 (2007) 21–27.
[17] J.C. Groen, S. Abelló, L.A. Villaescusa, J. Pérez-Ramírez, Mesoporous beta zeolite obtained by desilication original research article, Micropor. Mesopor. Mater. 114 (2008) 93–102.
[18] I. Schmidt, A. Krogh, K. Wienberg, A. Carlsson, M. Brorson, C.J.H. Jacobsen, Catalytic epoxidation of alkenes with hydrogen peroxide over first mesoporous titanium-containing zeolite, Chem. Commun. (2000) 2157–2158.
[19] I. Schmidt, A. Boisen, E. Gustavsson, K. Ståhl, S. Pehrson, S. Dahl, A. Carlsson, C.J.H. Jacobsen, Carbon nanotube templated growth of mesoporous zeolite single crystals, Chem. Mater. 13 (2001) 4416–4418.
[20] S.-S. Kim, J. Shah, T.J. Pinnavaia, Colloid-imprinted carbons as templates for the nanocasting synthesis of mesoporous ZSM-5 zeolite, Chem. Mater. 15 (2003) 1664–1668.
[21] Y. Fang, H. Hu, An ordered mesoporous aluminosilicate with completely crystalline zeolite wall structure, J. Am. Chem. Soc. 128 (2006) 10636–10637.
[22] Z.X. Yang, Y.D. Xia, R. Mokaya, Zeolite ZSM-5 with unique supermicropores synthesized using mesoporous carbon as a template, Adv. Mater. 16 (2004) 727–732.
[23] M. Choi, H. Sung Cho, R. Srivastava, C. Venkatesan, D.-H. Choi, R. Ryoo, Amphiphilic organosilane-directed synthesis of crystalline zeolite with tunable mesoporosity, Nat. Mater. 5 (2006) 718–723.
[24] H. Wang, T.J. Pinnavaia, MFI zeolite with small and uniform intracrystal mesopores, Angew. Chem. Int. Ed. 45 (2006) 7603–7606.
[25] J. Zhao, Z. Hua, Z. Liu, Y. Li, L. Guo, W. Bu, X. Cui, M. Ruan, H. Chen, J. Shi, Direct fabrication of mesoporous zeolite with a hollow capsular structure, Chem. Commun. (2009) 7578–7580.
[26] J.C. Groen, T. Bach, U. Ziese, A.M. Paulaime-van Donk, K.P. de Jong, J.A. Moulijn, J. Pérez-Ramírez, Creation of hollow zeolite architectures by controlled desilication of Al-zoned ZSM-5 crystals, J. Am. Chem. Soc. 127 (2005) 10792–10793.
[27] A. Bonilla, D. Baudouin, J. Perez-Ramirez, Desilication of ferrierite zeolite for porosity generation and improved effectiveness in polyethylene pyrolysis, J. Catal. 265 (2009) 170–180.
[28] J.C. Groen, L.A.A. Peffer, J.A. Moulijn, J. Pérez-Ramírez, On the introduction of intracrystalline mesoporosity in zeolites upon desilication in alkaline medium, Micropor. Mesopor. Mater. 69 (2004) 29–34.
[29] D.P. Serrano, J. Aguado, J.M. Escola, J.M. Rodríguez, A. Peral, Hierarchical zeolites with enhanced textural and catalytic properties synthesized from organofunctionalized seeds, Chem. Mater. 18 (2006) 2462–2464.
[30] Y. Tao, H. Kanoh, L. Abrams, K. Kaneko, Mesopore-modified zeolites: preparation, characterization, and applications, Chem. Rev. 106 (2006) 896–910.
[31] D.P. Serrano, J. Aguado, G. Morales, J.M. Rodríguez, A. Peral, M. Thommes, J.D. Epping, B.F. Chmelka, Molecular and meso- and macroscopic properties of hierarchical nanocrystalline ZSM-5 zeolite prepared by seed silanization, Chem. Mater. 21 (2009) 641–654.
[32] D.P. Serrano, J. Aguado, J.M. Escola, J.M. Rodríguez, A. Peral, Effect of the organic moiety nature on the synthesis of hierarchical ZSM-5 from silanized protozeolitic units, J. Mater. Chem. 18 (2008) 4210–4218.
[33] P.K. Ray, P.E. Montague, Crystallinity in jute fiber as revealed by multipeak resolution, J. Appl. Polym. Sci. 21 (1977) 1267–1272.
[34] K.S.W. Sing, Reporting physisorption data for gas/solid systems with special reference to the determination of surface area and porosity, Pure Appl. Chem. 54 (1982) 2201–2218.
[35] J. Pérez-Ramírez, D. Verboekend, A. Bonilla, S. Abelló, Zeolite catalysts with tunable hierarchy factor by pore-growth moderators, Adv. Funct. Mater. 19 (2009) 3972–3979.